Study of the microstructure resulting from brazed aluminium materials used in heat exchangers

J. Lacaze, S. Tierce, M.-C. Lafont, Y. Thebault, N. Pébère, G. Mankowski, C. Blanc, H. Robidou, D. Vaumousse and D. Daloz
CIRIMAT, UMR CNRS 5085, ENSIACET, 31077 Toulouse cedex 4, France
Valeo Engine Cooling, BP14, 72210 La Suze sur Sarthe, France
LSG2M, UMR CNRS 7584, ENSMN, 54042 Nancy cedex, France
Revised 22 June 2005. Available online 25 October 2005.

Abstract

Re-solidification of AA4343 cladding after brazing as well as the related precipitation in the modified AA3003 core material have been investigated. Analysis of the re-solidified material showed that partial dissolution of the core alloy occurs in both the brazing joints and away of them. Far from the brazing joints, the dissolution is, however, limited and diffusion of silicon from the liquid into the core material leads to solid-state precipitation in the so-called “band of dense precipitates” (BDP). On the contrary, the dissolution is enhanced in the brazing joint to such an extent that no BDP could be observed. The intermetallic phases present in the re-solidified areas as well as in the core material have been analyzed and found to be mainly cubic alpha-Al(Mn,Fe)Si. These results were then compared to predictions made with available phase diagram information.

Keywords: Aluminium materials; Heat exchangers; Microstructure; Brazing; Solidification

1. Introduction

Aluminium alloys are commonly used for heat exchangers in the automotive industry due to an interesting combination of properties (low density, good thermal conductivity, satisfactory mechanical properties and relatively good corrosion resistance). Since the middle of the 1990s, the trend with automotive heat exchangers is to replace mechanical assembly by brazing of aluminium alloys. This change is mainly due to cost and safety reasons as well as recycling issue. The present work was performed as part of a study devoted to the corrosion resistance of this generation of heat exchangers. The present brazed aluminium sheets consist of multi-layer materials made up of a core composed of a member of the 3XXX series clad on one or both sides with an alloy from the 4XXX series. The brazing process is based on the difference in the melting points of the core and of the cladding. During the brazing process, the parts to be assembled are heated for a short duration at a temperature between the melting temperatures of the two alloys. This process tends to modify the geometry and the microstructure of the cladding as well as the microstructure of the core. As it has been shown that partial dissolution of the core takes place in the brazing area [1], [2] and [3], the process must be tightly controlled. The formation of a “band

of dense precipitates" (BDP) in the core material due to the diffusion of Si coming from the liquid film has also been observed by several authors [2], [4] and [5]. The present work shows experimental observations on the microstructure resulting from re-solidification of the brazing material as well as from the solid-state transformations of the core material. Thermodynamic calculations carried out with available phase diagram information are then presented and compared with the observations.

2. Experimental procedure

Parts were cut from rolled modified AA3003 aluminium alloy (360 μm thick) clad on both faces with AA4343 aluminium alloy (20 μm thick). The parts were assembled after appropriate cutting, stamping and bending stages. The assembly obtained was submitted to industrial Nocolok® controlled atmosphere brazing (CAB). The maximum temperature was selected such as to be close to the liquidus temperature of AA4343, reported as 612 °C [6], while significantly below the solidus temperature of AA3003 that is about 640 °C [7]. The cooling rate was around 100 K min^{-1}. The microstructure of the alloys was examined both before and after brazing with optical microscopy (OM), scanning electron microscopy (SEM) with a JSM 6400 and transmission electron microscopy (TEM) with a JEM 2010. Both electron microscopes are equipped for energy dispersive spectrometry (EDS). EDS measurements were mainly made in spot mode to characterize the composition of individual phases. However, scanning mode was also used to estimate the nominal composition of the alloys by counting over appropriate "windows", 200 μm × 200 μm in size in the case of the core material, 10 μm × 200 μm for the cladding. In both spot mode and scanning mode, the counting time was 100 s. Apparent weight percentages obtained by EDS were afterwards corrected by means of a phi-rho-z software. The nominal composition of the two alloys estimated with EDS is given in Table 1.

Table 1.

Estimated compositions of the modified AA3003 core alloy and AA4343 cladding material (wt.%) used in this study

	Si	Mn	Fe	Cu	Zn	Al
Core alloy	0.08	1.10	0.16	0.19	0.1	Bal.
Cladding alloy	7.86	0.01	0.09	0.11	0.09	Bal.

3. Results

Fig. 1 and Fig. 2 show OM images of the sample section before brazing. Fig. 1a shows the initial assembly of the two parts to be joined where etching reveals the nearly uniform cladding that appears in white contrast while the core material has a grey colour with dark spots. The enlarged view in Fig. 2a reveals details of the microstructure of the two alloys when observed without chemical etching. In the cladding, elongated coarse particles with a dark grey contrast are precipitates of Si phase. SEM observations revealed also some small additional precipitates containing Al, Fe and Si. In the AA3003 core material, light grey particles are observed which were found with EDS to contain high levels of Al, Mn and Fe within a Al matrix (aluminium-rich fcc phase) that should be $Al_6(Mn,Fe)$ precipitates [8]. Owing to the low nominal silicon level of alloy AA3003, Si bearing intermetallic precipitates are not expected though they have been observed after homogenization at high temperature [8].

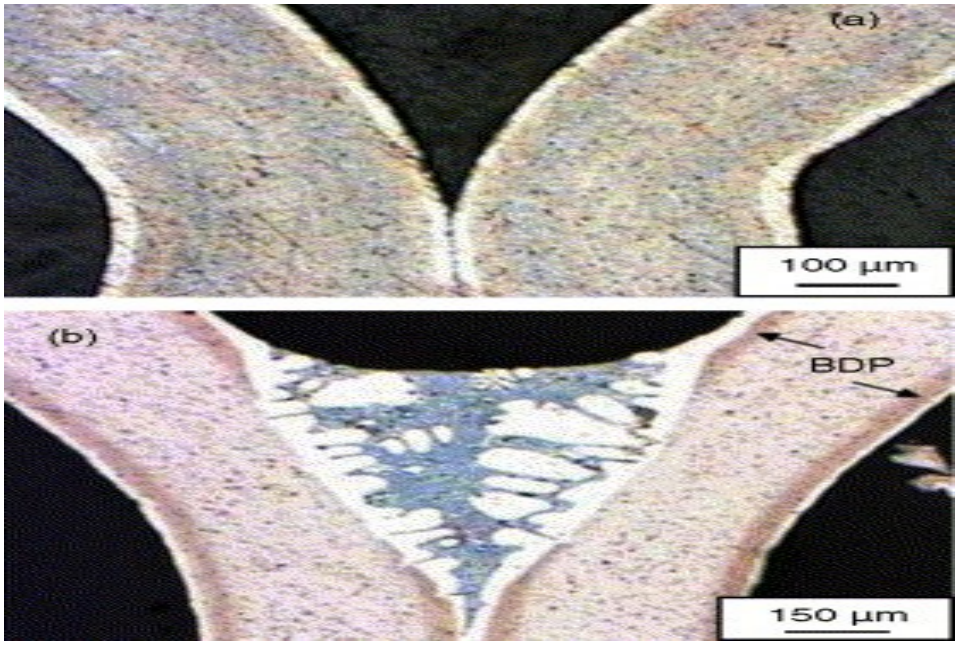

Fig. 1. OM images showing a metallographic section of an assembly before (a) and after (b) brazing. Keller's etching was used to reveal the structure.

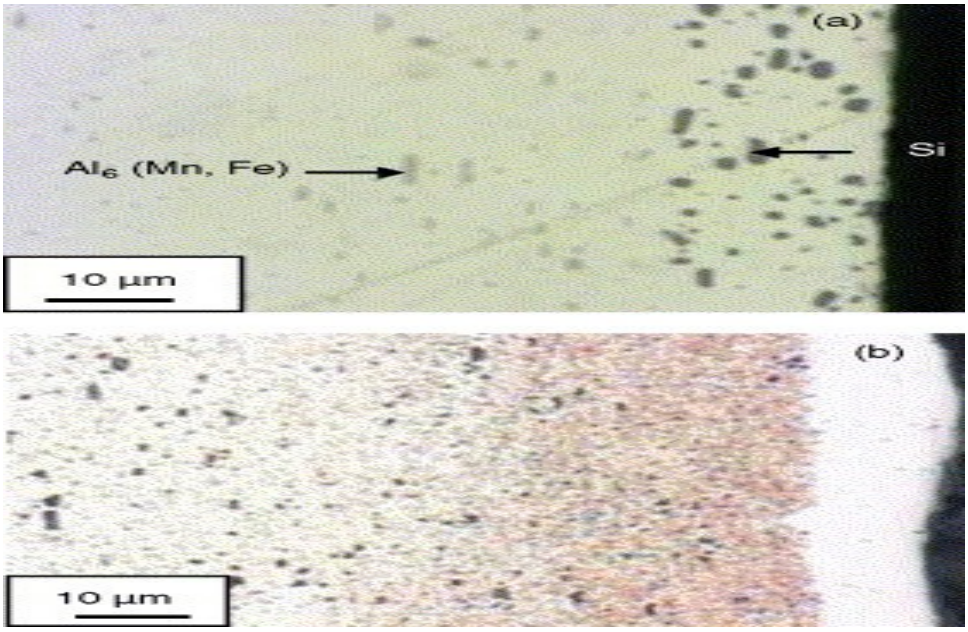

Fig. 2. Enlarged view (OM) of the material showing the microstructure of the cladding and of the core: (a) before brazing, no etching and (b) after brazing, far from the brazing joint, Keller's etching.

Fig. 1 and Fig. 2 show OM images of a metallographic section of the material after brazing. On both micrographs, the microstructure was revealed by etching with Keller's reactant. In Fig. 1b, re-solidification of the brazing joint shows up coarse dendrites of Al solid solution in white contrast and multiphase deposits in light grey contrast. The micrograph in Fig. 3 shows that these multiphase deposits consist of Al, Si that appears as elongated thin plates and more blocky precipitates. Close to the free surface of the brazing joint, large “Chinese-script” precipitates were also observed that form two-phase aggregates with Al. Both the blocky and “Chinese-script” precipitates were found to contain Al, Fe, Mn and Si as indicated by the measured compositions listed in Table 2.

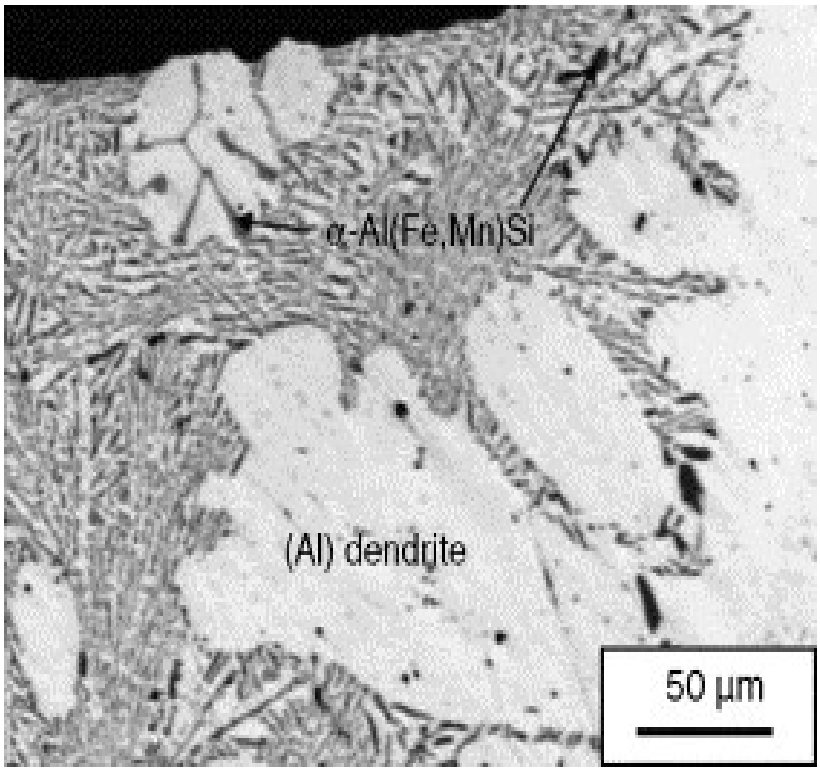

Fig. 3. OM image of the brazing joint.

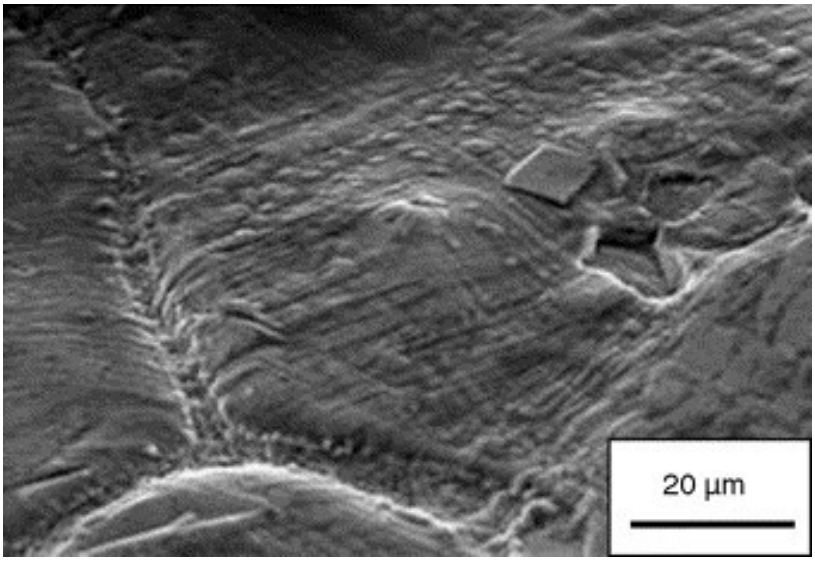

Fig. 4. SEM micrograph of the re-solidified cladding (SEI detector, 15 kV, 32 mm, tilt 45°).

Because dissolution of the core material occurs during the brazing process, attempt was made to measure the average Mn content in the brazing joint and in the re-solidified cladding material. However, this appeared unfeasible due to the fact that the microstructure is too coarse in both areas. Instead, an estimate of the Mn content in the liquid could be made by measuring the composition at the base of the Al dendrites and the grains assuming these locations correspond to the first solid to be formed upon re-solidification. The Mn content was found to be 0.25 wt.% in Al dendrites in the brazing joint and 0.07 wt.% in the grains. These values correspond to a significant Mn enrichment of the melt due to the dissolution of the core material. This enrichment is, however, much less pronounced away from the brazing joints, as conjectured from previous observations related to the formation of the BDP.

4. Discussion

In view of the above results, the first point to be discussed relates to the nature of the phase(s) containing Al, Fe, Si and Mn listed in Table 2. The early study of Munson [10] still appears as the most comprehensive one concerning the effect of Mn on intermetallic compounds containing Al, Fe and Si. The author showed first the composition domains in the ternary Al–Fe–Si system where Al_3Fe and various Al–Fe–Si compounds appear. Among these last ones, the most important for aluminium alloys are hexagonal α-AlFeSi and tetragonal (or monoclinic) β-AlFeSi which may precipitate through eutectic reaction with Al. When Mn is added at a level of 0.3 wt.%, Munson showed that a cubic α-AlMnFeSi phase is stabilized in place of the hexagonal α-AlFeSi, at least at low iron content. According to Barlock and Mondolfo [11], this phase is isomorphic with the cubic $Al_{15}Mn_3Si_2$ phase generally referred to as α-AlMnSi and thus appears as a ternary phase extending far in the quaternary system. It should thus be denoted α-Al(Fe,Mn)Si. Accordingly, X-ray diffraction was performed on the re-solidified cladding and clearly showed the presence of Al, Si and a cubic phase which could be indexed with the JCPDS data for the ternary α-AlMnSi phase (sheet 87-0528).

The compositions of the Al–Fe–Mn–Si precipitates given in the previous section (Table 2) are in good agreement with those reported for the α-Al(Fe,Mn)Si phase as reviewed by Balitchev et al. [12]. Most of the available data have been reported in Fig. 5 as Fe content versus Mn content [13], [14] and [15]. Results from Davignon et al. [13] show a nearly continuous series from the Al–Mn side to the Al–Fe side of the diagram, not depending on the fact that measurements were carried out on primary crystals (solid circles) or on "secondary" ones (empty circles). Results from Zakharov et al. [14] attributed to $Al_{16}(Fe,Mn)_4Si_3$ phase are also well in line with the whole set of data. Most of the available data show silicon content between 8 and 12 at.%, in quite good agreement with the values for the ternary phase in the Al–Mn–Si system for which the Si content varies from 9 to 13 at.% [16]. With the exception of measurements made on precipitates in the BDP which may have been affected by the surrounding matrix, results listed in Table 2 have been plotted in Fig. 5 with crosses for comparison. They show a good agreement with other values, leading to the conclusion that the four types of precipitates containing Al, Fe, Mn and Si are all cubic α-Al(Fe,Mn)Si phase isomorphic with α-AlMnSi phase.

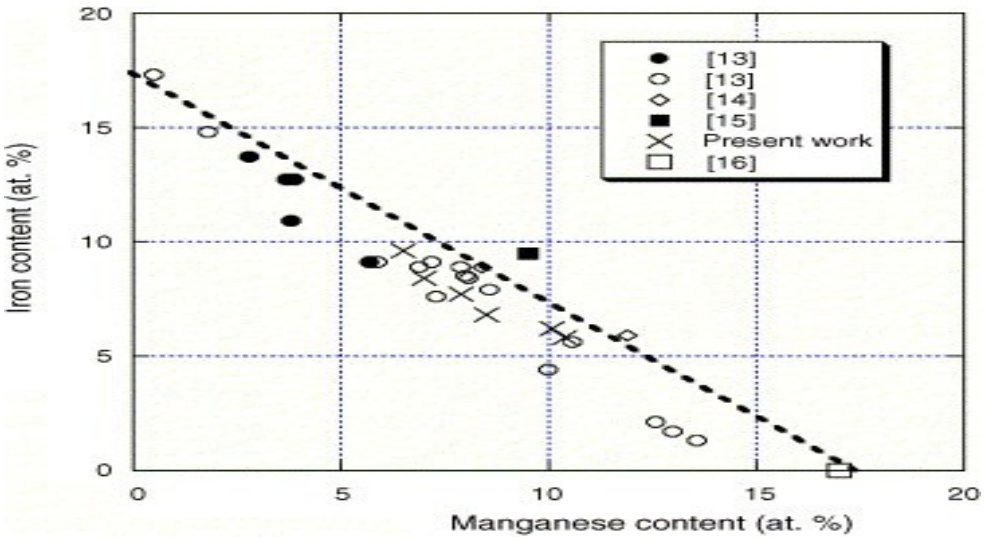

Fig. 5. Iron vs. manganese content of the α-Al(Fe,Mn)Si phase as reported in the literature and as measured in the present study. The dotted line corresponds to the stoichiometry selected in the Al data base [19], $Al_{32}(Fe,Mn)_8(Al,Si)_4Si_2$.

The COST 507 data base for aluminium and light alloys [17] provides Gibbs energy description following the so-called CALPHAD method limited to ternary systems. It proved to be useful for a first check of the present results with thermodynamic information [18]. However, the solidification path could not be predicted with certainty because the description of the cubic α-AlMnSi phase does not account for substitution of Fe to Mn in this data base. It was thus decided to resort to the Al data base developed by Saunders in which this has been described, though no information is available on the data considered for optimization of the parameters [19]. In this base, the α-AlMnSi phase is described as $Al_{32}(Fe,Mn)_8(Al,Si)_4Si_2$. All the calculations were performed with the THERMOCALC software [20]. Fig. 6 shows part of the isopleth Al–Si sections of the Al–Fe–Mn–Si system at 0.1 wt.% Fe, and either 0.15 wt.% Mn (Fig. 6a) or 0.5 wt.% Mn (Fig. 6b). The Mn contents correspond to the composition evaluated for the remaining liquid from the composition of the Al phase, respectively, on the flat surfaces and in the brazing joint. It is seen that Mn strongly stabilizes the cubic α-Al(Fe,Mn)Si phase although the solidification path of alloys with about 8 wt.% silicon should anyway start with precipitation of Al. It is worth mentioning that 0.15 wt.% Mn is predicted to be sufficient for the α-Al(Fe,Mn)Si phase while Munson [10] indicated a minimum level of 0.30 wt.%.

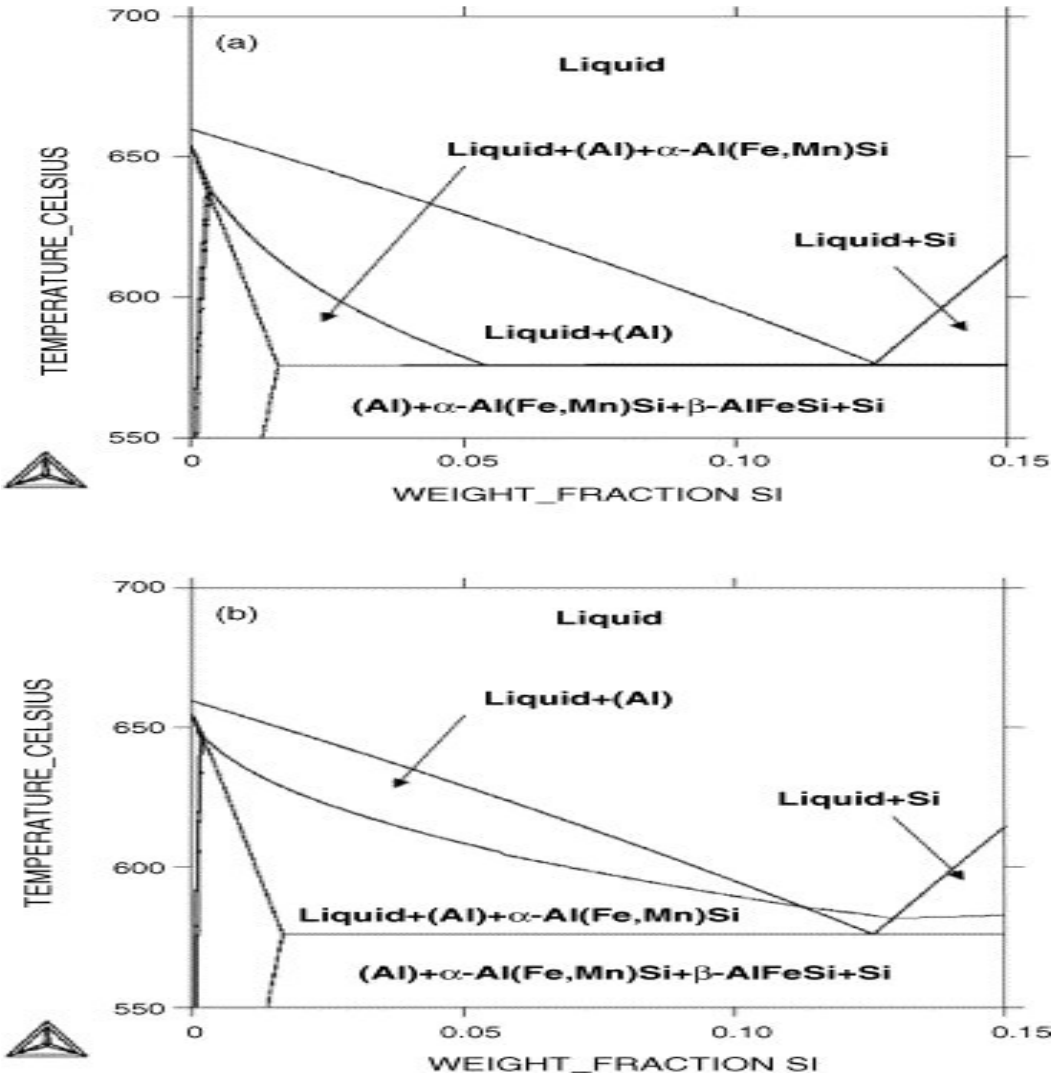

Fig. 6. Part of the Al–Si isopleth section of the Al–Fe–Mn–Si phase diagram calculated for 0.1 wt.% Fe and either 0.15 wt.% Mn (a) or 0.5 wt.% Mn (b).

Solidification kinetics following the Scheil's model [21] was then calculated for both alloys using the ad hoc module of THERMOCALC (see Fig. 7). During solidification, it is predicted that the sequence of solid phases appearing should be Al/Si/α-Al(Fe,Mn)Si and Al/α-Al(Fe,Mn)Si/Si for the molten cladding and the brazing joints, respectively. The difference in sequence is in agreement with the difference in the microstructures observed, namely the observation of two phase aggregates with Al and α-Al(Fe,Mn)Si in the brazing joint and not in the re-solidified layer. It is worth noting that the solidification kinetics are quite similar although the solidification sequences are different. This is due to the fact that the amount of the second phase to appear, Si or α-Al(Fe,Mn)Si, is in any case very low. Also, it should be mentioned that a very low amount of β-AlFeSi phase is in fact predicted at the very end of the solidification of the re-solidified layer but has not been observed. This may be due to some back diffusion of solutes during solidification or to nucleation kinetics of this phase. Finally, the origin of the plates of α-Al(Fe,Mn)Si phase seen at the surface or sub-surface of the re-solidified layer does not fit the predicted solidification path and should be further investigated.

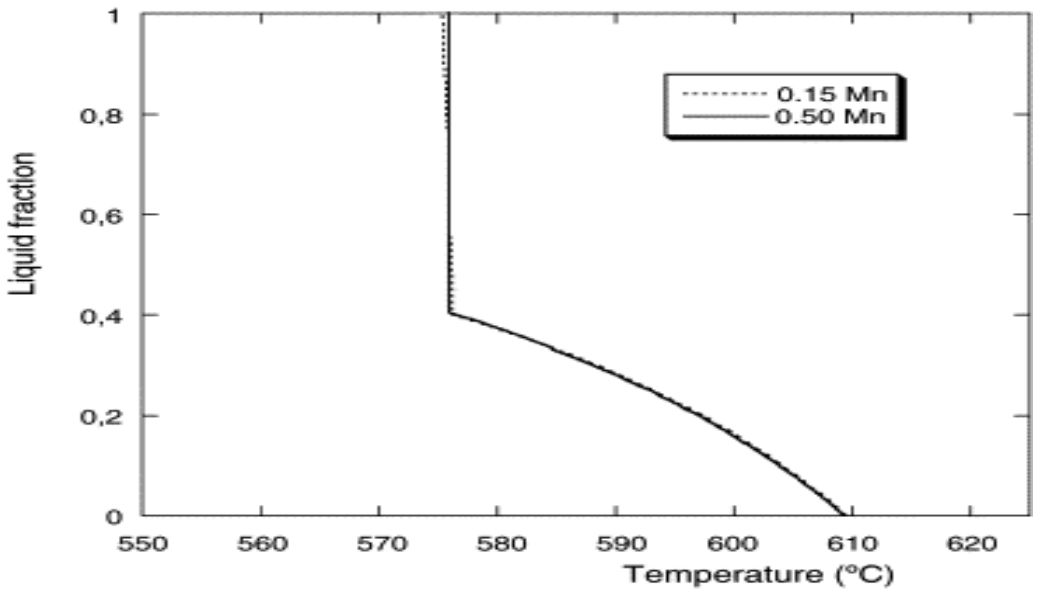

Fig. 7. Solidification kinetics according to the Scheil's model for alloys with 8 wt.% Si, 0.1 wt.% Fe and either 0.15 wt.% Mn (- - -) or 0.5 wt.% Mn (—).

5. Conclusion

Two distinct regions are subject to microstructural evolution during the brazing process: the brazing joint and the molten cladding with the solid diffusion zone next to it. The present characterizations of both regions show that they are composed of Al, Si and a third phase that has been identified as α-Al(Fe,Mn)Si. In the brazing joint, extended dissolution of modified AA3003 occurs and leads to an enrichment in Mn of the liquid. The microstructure observed in this zone is in good agreement with the solidification path determined via phase diagram computation, i.e. Al, Al + α-Al(Fe,Mn)Si then Al + α-Al(Fe,Mn)Si + Si.

In the molten cladding lower enrichment in Mn is noticed and leads to a different calculated solidification path: Al, Al + Si, Al + Si + α-Al(Fe,Mn)Si + β-AlFeSi. The predicted initial deposit of Al + Si eutectic in this case is in agreement with the inexistence of two-phase aggregates of Al and α-Al(Fe,Mn)Si in the re-solidified cladding. The origin of plate-like α-Al(Fe,Mn)Si observed at the surface of the re-solidified layer or embedded in the Al grains should be clarified.

References

M. Nylen, U. Gustavsson, B. Hutchinson, A. Ortnas, J.H. Driver, et al. (Eds.), Aluminium Alloys, Proceedings of ICAA5, Materials Science Forum, vol. 217–222, Trans. Tech. Publication, Zürich, 1996, p. 1703.

In: R.A. Woods, Editor, *VTMS3: Conference Proceedings 1997 Vehicle Thermal Management Systems, vol. 314*, SAE, Warrendale (1997), p. 639.

In: H.J. Yang and R.A. Woods, Editors, *Conference Proceedings 1997 Vehicle Thermal*

Management Systems, vol. 314, SAE, Warrendale (1997), p. 649.

G.J. Marshall, R.K. Bolingbroke and A. Gray, *Metall. Trans. A* **24** (1993), p. 1935.

R. Benedictus, S.D. Meijers, A.J. Wittebrood and J.H.W. de Witt, *Aluminium Alloys* **3** (1998), p. 1577.

R. Delevay, Techniques de l'ingénieur, M 440, p. 42.

Metals Handbook, Properties and Selection of Metals, ASM International, vol. 1, eighth ed., Metals Park, 1961, p. 940.

Y.J. Li and L. Arnberg, *Mater. Sci. Eng. A* **347** (2003), p. 130.

D.T.L. Alexandre and A.L. Greer, *Acta Mater.* **50** (2002), p. 2571.

D.J. Munson, *Inst. Met.* **95** (1967), p. 217.

J.G. Barlock and L.F. Mondolfo, *Z. Metallkde.* **66** (1975), p. 605.

E. Balitchev, T. Jantzen, I. Hurtado and D. Neuschutz, *Computer Coupling of Phase Diagrams Thermochem.* **27** (2003), p. 275.

G. Davignon, A. Serneels, B. Verlinden and L. Delaey, *Metall. Mater. Trans. A* **27** (1996), p. 3357.

A.M. Zakharov, I.T. Gul'din, A.A. Arnol'd and Yu.A. Matsenko, *Russ. Metall.* **4** (1989), p. 209. Cited By in Scopus (0)

M.V. Kral, H.R. McIntyre and M.J. Smillie, *Scr. Mater.* **51** (2004), p. 215.

N. Krendelsberger, F. Weitzer and J.C. Schuster, *Metall. Mater. Trans. A* **33** (2002), p. 3311.

Thermochemical Database for Light Metal Alloys, first ed. Ansara, European Commission, Bruxelles, 1995; COST 507, European Commission, EUR 18171, 18499 and 18475, Bruxelles, 1998.

S. Tierce, N. Pébère, C. Blanc, G. Mankowski, H. Robidou, D. Vaumousse and J. Lacaze, *Int. Cast Metals Res. J.* **18** (2005), pp. 370–376.

N. Saunders (Ed.), in: Aluminium Alloys, Proceedings of ICAA5, Materials Science Forum, vol. 217–222, Trans. Tech. Publication, 1996, p. 667.

B. Sundman and B. Jansson, *CALPHAD* **9** (1985), p. 153.

M.C. Flemings, Solidification Processing, McGraw Hill, New-York (1974).

Corresponding author. Tel.: +33 5 6288 5710; fax: +33 5 6288 5663.